Anomalous suppression of the superfluid density in the Cu$_x$Bi$_2$Se$_3$ superconductor upon progressive Cu intercalation

M. Kriener, Kouji Segawa, Satoshi Sasaki, and Yoichi Ando

Institute of Scientific and Industrial Research, Ibaraki, Osaka University, Osaka 567-0047, Japan
(Received 27 June 2012; published 19 November 2012)

Cu$_x$Bi$_2$Se$_3$ was recently found to be likely the first example of a time-reversal-invariant topological superconductor accompanied by helical Majorana fermions on the surface. Here we present that progressive Cu intercalation into this system introduces significant disorder and leads to an anomalous suppression of the superfluid density which was obtained from the measurements of the lower critical field. At the same time, the transition temperature T_c is only moderately suppressed, which agrees with a recent prediction for the impurity effect in this class of topological superconductors bearing strong spin-orbit coupling. Those unusual disorder effects give support to the possible odd-parity pairing state in Cu$_x$Bi$_2$Se$_3$.

A topological superconductor (TSC) is a superconducting analog of topological insulators (TIs) and is characterized by a nontrivial topological structure of the Hilbert space, which is specified by nontrivial Z or Z_2 indices.[1–7] Its hallmark signature is the appearance of surface Majorana fermions, which are their own antiparticles and are of fundamental intellectual interest.[8] Recently, it was theoretically predicted[9] and experimentally confirmed[10] that a superconducting doped TI material Cu$_x$Bi$_2$Se$_3$ is likely the first concrete example of a time-reversal-invariant TSC. Its parent TI material Bi$_2$Se$_3$ consists of basic crystallographic units of Se-Bi-Se-Bi-Se quintuple layers, which are weakly bonded by the van der Waals force. Upon intercalation of Cu into the van der Waals gap, superconductivity appears below the critical temperature T_c of up to ∼3.8 K.[11] This is high for its low charge carrier concentration of only ∼10^{20} cm^{-3}.[11] As a "superconducting topological insulator," this material has attracted a great deal of interest.[9,12–26]

Unfortunately, Cu$_x$Bi$_2$Se$_3$ has a materials problem in that samples with a large superconducting volume fraction are difficult to obtain with the usual melt-growth method,[11,12] which has hindered detailed studies of the superconducting properties of this material. However, this problem has been ameliorated recently by the development of an electrochemical synthesis technique[18] which allowed the synthesis of superconducting samples with the shielding fraction exceeding 50%.[17] Such an improvement made it possible to perform point-contact spectroscopy on a cleaved surface of Cu$_x$Bi$_2$Se$_3$ to find a signature of the Andreev bound state in the form of a pronounced zero-bias conductance peak,[10] which gives evidence for unconventional superconductivity.[27,28] Knowing that the symmetry of this material[29,30] allows only four types of superconducting gap functions[9] and that all possible unconventional states are topological,[10] it was possible to conclude that Cu$_x$Bi$_2$Se$_3$ is most likely a TSC.[10]

Although the point-contact spectroscopy elucidated the possible TSC nature of Cu$_x$Bi$_2$Se$_3$, the electron mean free path ℓ in the superconducting samples of this material is comparable to the coherence length ξ_0;[17] according to the common belief,[31,32] the odd-parity pairing should be strongly suppressed by impurity scattering in such a situation.[33,34] In this context, a recent theory by Michaeli and Fu addressed this issue[23] and showed that odd-parity superconductivity

in strongly spin-orbit coupled semiconductors such as Cu$_x$Bi$_2$Se$_3$ are much more robust against the pair-breaking effect induced by impurity scattering than in more ordinary odd-parity superconductors. Therefore, thanks to the role of spin-orbit coupling, T_c of Cu$_x$Bi$_2$Se$_3$ is expected to be rather insensitive to nonmagnetic impurities, which is similar to conventional superconductors.[35]

In this Rapid Communication, we address the issue of disorder effects in Cu$_x$Bi$_2$Se$_3$. Through our systematic studies of the effects of Cu intercalation in this system, it turned out that increasing the Cu content beyond $x \sim 0.3$ in the superconducting regime does not increase T_c or the carrier concentration, but its main effect is to enhance the residual resistivity ρ_0. This suggests that one can consider the Cu content x to be a parameter to control the disorder while keeping other fundamental parameters virtually unchanged. By looking at the data from this perspective, the x dependence of the superfluid density obtained from the lower critical field shows an unusual disorder dependence that is distinct from that in conventional BCS superconductors, which gives support to unconventional pairing. In addition, we show that the x dependence of T_c is essentially a reflection of the disorder effect and is consistent with the particular odd-parity paring state that is supposed to be realized in Cu$_x$Bi$_2$Se$_3$.

Cu$_x$Bi$_2$Se$_3$ single crystals of slablike geometry with various Cu contents $0.11 \leqslant x \leqslant 0.50$ were prepared by the electrochemical technique described earlier.[18] The typical sample size was $4 \times 2.5 \times 0.3$ mm^3. The magnetic field dependence of the magnetization $M(B)$ were measured with a commercial superconducting quantum interference device (SQUID) magnetometer (Quantum Design MPMS) with particular attention being paid to the low-field regime.[36] Roughly half of the samples were also characterized by transport measurements by a standard six-probe method. Figure 1 summarizes the x dependences of T_c, ρ_0 (defined as ρ at $T = 5$ K), the superconducting shielding fraction at $T = 1.8$ K, and the charge carrier concentration n (determined from the Hall coefficient at 5 K). Most notably, ρ_0 strongly increases for $x > 0.3$ and n is basically independent of x at $n \simeq 1.5 \times 10^{20}$ cm^{-3}.[37]

Before presenting magnetic properties, we define and summarize important parameters. The layered structure of Cu$_x$Bi$_2$Se$_3$ leads to anisotropies in the superconducting
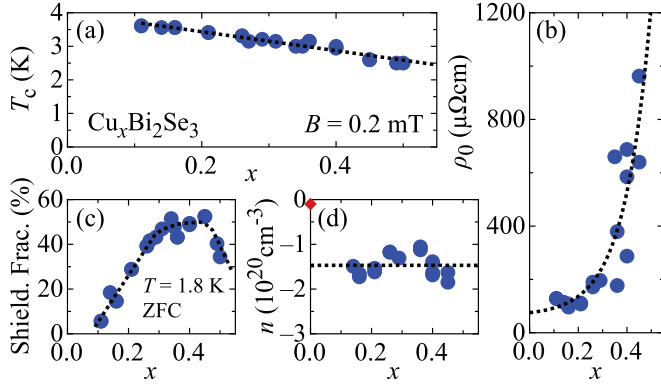
FIG. 1. (Color online) Cu content x dependences of (a) critical temperature T_c, (b) residual resistivity ρ_0, (c) superconducting shielding fraction, and (d) normal-state carrier density n. For comparison, the carrier density in pristine Bi_2Se_3 ($\lesssim 10^{19}$ cm^{-3}) is shown with a diamond. Note that n is essentially x independent and remains low at $\sim 1.5 \times 10^{20}$ cm^{-3}. The dotted lines are guides to the eyes.

parameters, and we denote the lower and upper critical fields for magnetic fields parallel and perpendicular to the crystallographic ab planes as $B_{c1,ab}$, $B_{c1,c}$, $B_{c2,ab}$, and $B_{c2,c}$, respectively. Also, the penetration depths and the coherence lengths along the in-plane and out-of-plane directions are denoted as λ_{ab}, λ_c, ξ_{ab}, and ξ_c, respectively. The anisotropic Ginzburg-Landau parameters are defined as $\kappa_{ab} = \sqrt{\lambda_{ab}\lambda_c/(\xi_{ab}\xi_c)}$ and $\kappa_c = \lambda_{ab}/\xi_{ab}$.[38–40] The upper critical fields are related to the coherence lengths via $B_{c2,ab} = \Phi_0/2\pi\xi_{ab}\xi_c$ and $B_{c2,c} = \Phi_0/2\pi\xi_{ab}^2$ with the flux quantum Φ_0. In the Ginzburg-Landau theory, B_{c1} is related to the vortex line energy E via $B_{c1} = 4\pi\mu_0 E/\Phi_0$;[41] for extremely type-II superconductors with $\kappa \gg 1$, one obtains $E \approx [\Phi_0^2/(4\pi\lambda)^2]\ln\kappa$. However, to take into account the vortex core energy, the $\ln\kappa$ term has to be corrected by adding 0.5,[42–44] and the formula for $B_{c1,ab}$ becomes

$$B_{c1,ab} = \frac{\Phi_0}{4\pi}[\ln(\kappa_{ab}) + 0.5]\frac{1}{\lambda_{ab}\lambda_c}. \quad (1)$$

Hence, to calculate the Ginzburg-Landau parameter κ_{ab}, we use $B_{c1,ab}/B_{c2,ab} = (\ln\kappa_{ab} + 0.5)/2\kappa_{ab}^2$. The anisotropy factor is defined as $\gamma \equiv B_{c2,ab}/B_{c2,c} = B_{c1,c}/B_{c1,ab} = \lambda_c/\lambda_{ab}$ and the penetration depths are determined by solving Eq. (1) for λ_{ab} by using $\lambda_c = \gamma\lambda_{ab}$. For the following discussion, we define the averaged penetration depth $\lambda_{av} = \sqrt[3]{\lambda_{ab}^2\lambda_c}$, which allows the calculation of the superfluid density via $n_s = m^*/(\mu_0 e^2\lambda_{av}^2)$ with the effective mass m^* assumed to be x independent.[45]

Figure 2 describes how $B_{c1,ab}$ is determined from the magnetization data M_{exp}, which is essentially the same as was done in Ref. 17. Figure 2(a) shows $M_{exp}(B)$ curves for a sample with $x = 0.26$ at various temperatures between 1.8 and 3.0 K; the T_c of this sample was ~ 3.2 K. The dashed line M_{lin} is a fit to the low-field magnetization at 1.8 K, representing the initial Meissner screening. Determining such a linear part for each temperature and subtracting it from the $M_{exp}(B)$ data yields $\Delta M = M_{exp} - M_{lin}$, which is shown in Fig. 2(b) (the data are shifted for clarity). The arrows mark the last field above which ΔM shows an obvious deviation from zero (i.e., ΔM becomes $\gtrsim 0.02$), signaling the entry of vortices and defining the flux entry field $B_1(T)$. These data
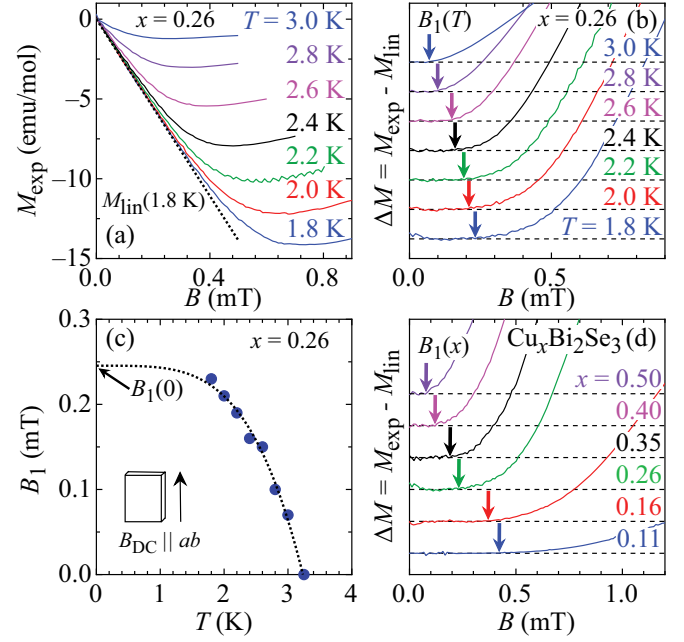

FIG. 2. (Color online) (a) Initial low-field M_{exp} vs B curves for a sample with $x = 0.26$ at various temperatures. (b) Reduced magnetization ΔM after subtracting the initial linear Meissner contribution M_{lin}. The deviation points marked by arrows indicate B_1 at each temperature. (c) Plot of B_1 vs T for $x = 0.26$ together with a fit to the data. (d) Plots of ΔM vs B at 1.8 K for various x.

points are plotted as B_1 vs T in Fig. 2(c) and are fitted with the empirical formula $B_1(T) = B_1(0)[1 - (T/T_c)^4]$.[46] Sometimes the $B_1(T)$ data scatter around the fitting line, which leads to a sample-dependent error bar on $B_1(0)$. To show the trend of how B_1 changes with the Cu concentration x, the 1.8-K magnetization data for various x are shown in Fig. 2(d); this plot clearly suggests that $B_1(0)$ becomes systematically smaller for larger x.

To determine B_{c1} from B_1, one should consider the influences of the demagnetization effect, the surface quality (Bean-Livingston surface barrier), and the bulk pinning effects. The surface barrier is not effective in rough surfaces, which is the case in all of our as-grown samples (see Fig. S4 of Ref. 10) irrespective of the x values, and the bulk pinning is also extremely weak in $Cu_xBi_2Se_3$, as indicated by magnetic hysteresis data.[17,47] As for the demagnetization effect, albeit small ($<10\%$) in the present case, we have corrected for it by using the Brandt's formula for slab-shaped samples with an aspect ratio b/a:[48] $B_{c1}(0) = B_1(0)/\tanh\sqrt{0.36\,b/a}$. The obtained B_{c1} for all samples are plotted vs x in Fig. 3(a). The corresponding λ_{av} values are shown in Fig. 3(b); for calculating λ_{av}, we need the anisotropy factor γ which was obtained from anisotropic B_{c2} determined from the resistive transitions in magnetic fields applied parallel and perpendicular to the ab plane [Fig. 3(c)]. The obtained γ is essentially independent of x [Fig. 3(d)], which supports the idea that the main effect of Cu intercalation beyond $x \sim 0.3$ is to enhance the disorder without changing band structure or mobile carrier density.

As already mentioned, the averaged penetration depth λ_{av} directly gives the superfluid density $n_s = m^*/(\mu_0 e^2\lambda_{av}^2)$.[49] We normalize this value with the normal-state carrier density n,
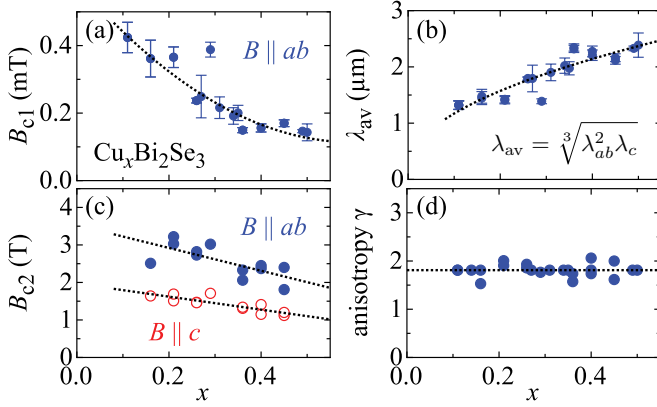
FIG. 3. (Color online) x dependences of (a) $B_{c1}(0)$ for $B \parallel ab$ after the demagnetization correction, (b) corresponding penetration depth λ_{av}, (c) $B_{c2}(0)$ for fields parallel and perpendicular to the ab planes, and (d) anisotropy factor γ. Dotted lines are guides to the eyes.

and Fig. 4(a) summarizes the x dependence of $n_s^{exp} \equiv n_s/n$. One can see that n_s/n is already only 0.3 at $x \simeq 0.10$ where the superconductivity starts to appear, and it is further suppressed with increasing x. This behavior is obviously a reflection of strong disorder caused by Cu intercalation that can be inferred in Fig. 1(b). Since it is known that disorder causes a reduction in n_s even in conventional BCS superconductors,[50,51] it is prudent to discuss this behavior quantitatively.

According to Anderson's theorem,[35] the superconducting gap Δ_0 and T_c of conventional superconductors are relatively insensitive to small concentrations of nonmagnetic impurities. However, the superfluid density, which reflects the "rigidity" of the electronic system to electromagnetic perturbations, is
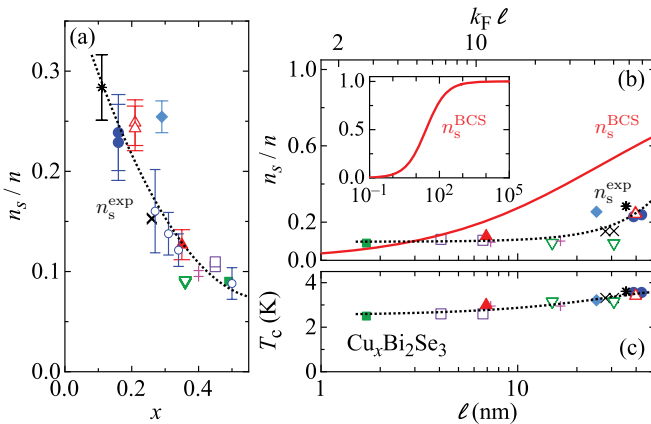

FIG. 4. (Color online) (a) Normalized superfluid density n_s/n vs x, with n the normal-state carrier density. For symbols without error bars, the estimated errors are smaller than the symbol size. (b), (c) Semilog plots of n_s/n (b) and T_c (c) vs the mean free path ℓ. The upper axis gives the corresponding $k_F\ell$ value. To facilitate comparisons between (a) and (b) [(c)], data for different x values are indicated by different symbols. The solid line n_s^{BCS} in (b) gives the expected disorder-induced suppression of n_s/n for a conventional BCS superconductor. The inset shows $n_s^{BCS} \to 1$ in the clean limit $\ell \to \infty$. The dotted lines in all panels are guides to the eyes.

affected by disorder in conventional superconductors.[50–52] Indeed, the disorder dependence of n_s has been studied in Nb and Pb and was found to follow the theoretical prediction.[53,54] We therefore compare the disorder dependence of n_s observed in $Cu_xBi_2Se_3$ to the expectation for ordinary BCS superconductors. For such a comparison, one needs to parametrize disorder, which is usually done by evaluating $k_F\ell$, where $k_F = \sqrt[3]{3\pi^2 n}$ is the Fermi wave number[55] and $\ell = \hbar k_F/(\rho_0 n e^2)$ is the mean free path.[56]

For a pure BCS superconductor, the penetration depth in the 0-K limit is given by $\lambda_L^2(0) = m^*/(\mu_0 e^2 n)$, because n_s is equal to n in the clean limit. In the presence of disorder, this $\lambda_L(0)$ in the clean limit is modified to an effective penetration depth which is evaluated at $T = 0$ K as $\lambda_{BCS}(0) = \lambda_L(0)\sqrt{1 + \xi_0/\ell} > \lambda_L(0)$ in the local limit,[57,58] where $\xi_0 = \hbar v_F/(\pi \Delta_0)$ is the Pippard coherence length for pure superconductors ($v_F = \hbar k_F/m^*$ is the Fermi velocity and Δ_0 is the BCS gap).[59] From this $\lambda_{BCS}(0)$ we calculate the superfluid density $n_s^{BCS}(\ell)$, which gives the disorder-induced suppression of n_s for a conventional BCS superconductor.

Figure 4(b) shows the comparison of the ℓ dependences of n_s^{exp} and n_s^{BCS} ($k_F\ell$ value is shown in the upper axis). In this figure, the BCS calculation is shown as a solid line and the inset shows the saturation of $n_s^{BCS} \to 1$ in the clean limit $\ell \to \infty$. Clearly, n_s^{exp} does not agree with n_s^{BCS}; although both are suppressed with decreasing ℓ, the suppression is much stronger in $Cu_xBi_2Se_3$ than is expected for a BCS superconductor. Also, it is useful to compare the result shown in Fig. 4(b) to that in Fig. 1(b): At $x > 0.3$, the residual resistivity starts to increase drastically and ℓ becomes shorter than $\sim$25 nm; however, n_s^{exp} tends to saturate in this dirtier range of $\ell < 25$ nm. Moreover, for $\ell < 4$ nm, n_s^{exp} intersects the n_s^{BCS} curve. Hence, both the strong suppression in the intermediate disorder regime and the saturation tendency in the dirtier regime are anomalous. Such an anomalous behavior of n_s/n is the main result of this work, and it naturally points to an unconventional nature of the superconducting state in $Cu_xBi_2Se_3$.

In contrast to the highly anomalous behavior of n_s^{exp}, the modest suppression of T_c shown in Fig. 4(c) resembles the behavior of dirty conventional superconductors.[35] One might hasten to conclude that such an ordinary disorder dependence of T_c speaks against the odd-parity pairing, because the common belief for odd-parity superconductors is that T_c is quickly suppressed with impurity-induced disorder.[31,32] However, as we already mentioned above, the particular type of odd-parity pairing that is considered to be realized in $Cu_xBi_2Se_3$ (Refs. 9 and 10) belies this common belief. This point was recently shown by Michaeli and Fu,[23] who analyzed the novel interorbital, odd-parity state[9] proposed for $Cu_xBi_2Se_3$. The odd-parity pairing takes place between two p_z orbitals with different parity at the upper and lower ends of the quintuple layers via attractive short-range interactions. In such a state, the crucial disorder-induced pair breaking effect is significantly suppressed as a result of strong spin-momentum locking. The dephasing rate of the Cooper pairs depends on the ratio of band mass and chemical potential, m/μ; as this ratio becomes smaller, the superconductivity becomes more robust. For $Cu_xBi_2Se_3$, this ratio has been estimated[19] to be $\sim$1/3 and

the calculated T_c depends only weakly on the impurity-induced disorder,[23] in qualitative agreement with Fig. 4(c). Therefore, the observed disorder effect in T_c is not inconsistent with the odd-parity pairing.

To summarize, we report an anomalous suppression of the superfluid density n_s/n probed by the lower critical field as a function of the Cu content x. Since it appears that the main effect of Cu intercalation beyond $x \sim 0.3$ is to enhance disorder without significantly changing band structure or carrier density, our result reveals the impact of disorder on the superconducting state in $Cu_xBi_2Se_3$. Most strikingly, in the intermediate range of disorder, n_s/n is much more strongly suppressed than is expected for a dirty conventional BCS superconductor, while in the strongly disordered regime n_s/n

tends to saturate. In contrast, the occurrence of superconductivity itself is robust against disorder, as indicated by an only moderate suppression of T_c with x. The obviously anomalous behavior in n_s/n points to an unconventional pairing state, and the ostensibly normal behavior in T_c is consistent with the theoretically-proposed odd-parity pairing state with strong spin-momentum locking. Altogether, our result gives support to the possible odd-parity pairing state in $Cu_xBi_2Se_3$.

[1] L. Fu and C. L. Kane, Phys. Rev. Lett. **100**, 096407 (2008).

[2] A. P. Schnyder, S. Ryu, A. Furusaki, and A. W. W. Ludwig, Phys. Rev. B **78**, 195125 (2008).

[3] X.-L. Qi, T. L. Hughes, S. Raghu, and S.-C. Zhang, Phys. Rev. Lett. **102**, 187001 (2009).

[4] X.-L. Qi, T. L. Hughes, and S.-C. Zhang, Phys. Rev. B **81**, 134508 (2010).

[5] J. Linder, Y. Tanaka, T. Yokoyama, A. Sudbø, and N. Nagaosa, Phys. Rev. Lett. **104**, 067001 (2010).

[6] M. Sato, Phys. Rev. B **81**, 220504(R) (2010).

[7] X.-L. Qi and S.-C. Zhang, Rev. Mod. Phys. **83**, 1057 (2011).

[8] F. Wilczek, Nat. Phys. **5**, 614 (2009).

[9] L. Fu and E. Berg, Phys. Rev. Lett. **105**, 097001 (2010).

[10] S. Sasaki, M. Kriener, K. Segawa, K. Yada, Y. Tanaka, M. Sato, and Y. Ando, Phys. Rev. Lett. **107**, 217001 (2011).

[11] Y. S. Hor, A. J. Williams, J. G. Checkelsky, P. Roushan, J. Seo, Q. Xu, H. W. Zandbergen, A. Yazdani, N. P. Ong, and R. J. Cava, Phys. Rev. Lett. **104**, 057001 (2010).

[12] L. A. Wray, S.-Y. Xu, Y. Xia, Y. S. Hor, D. Qian, A. V. Fedorov, H. Lin, A. Bansil, R. J. Cava, and M. Z. Hasan, Nat. Phys. **6**, 855 (2010).

[13] P. Das, Y. Suzuki, M. Tachiki, and K. Kadowaki, Phys. Rev. B **83**, 220513(R) (2011). In this paper the authors argue that a magnetic field created inside a vortex leads to a polarization of the spins forming the spin-triplet pairs in $Cu_xBi_2Se_3$ and hence a nonuniform spin magnetization in the sample. This is in contradiction to the nonmagnetic, time-reversal-invariant pairing state discussed for $Cu_xBi_2Se_3$, which consists of Cooper pairs with zero total angular momentum (see Refs. 9 and 19).

[14] L. Hao and T. K. Lee, Phys. Rev. B **83**, 134516 (2011).

[15] Y. Ishida, H. Kanto, A. Kikkawa, Y. Taguchi, Y. Ito, Y. Ota, K. Okazaki, W. Malaeb, M. Mulazzi, M. Okawa, S. Watanabe, C.-T. Chen, M. Kim, C. Bell, Y. Kozuka, H. Y. Hwang, Y. Tokura, and S. Shin, Phys. Rev. Lett. **107**, 077601 (2011).

[16] T. Kirzhner, E. Lahoud, K. B. Chaska, Z. Salman, and A. Kanigel, Phys. Rev. B **86**, 064517 (2012).

[17] M. Kriener, K. Segawa, Z. Ren, S. Sasaki, and Y. Ando, Phys. Rev. Lett. **106**, 127004 (2011).

[18] M. Kriener, K. Segawa, Z. Ren, S. Sasaki, S. Wada, S. Kuwabata, and Y. Ando, Phys. Rev. B **84**, 054513 (2011).

[19] L. A. Wray, S. Xu, Y. Xia, D. Qian, A. V. Fedorov, H. Lin, A. Bansil, L. Fu, Y. S. Hor, R. J. Cava, and M. Z. Hasan, Phys. Rev. B **83**, 224516 (2011).

[20] T. V. Bay, T. Naka, Y. K. Huang, H. Luigjes, M. S. Golden, and A. de Visser, Phys. Rev. Lett. **108**, 057001 (2012).

[21] J. Alicea, Rep. Prog. Phys. **75**, 076501 (2012); C. W. J. Beenakker, arXiv:1112.1950.

[22] T. H. Hsieh and L. Fu, Phys. Rev. Lett. **108**, 107005 (2012).

[23] K. Michaeli and L. Fu, Phys. Rev. Lett. **109**, 187003 (2012).

[24] Y. Tanaka, M. Sato, and N. Nagaosa, J. Phys. Soc. Jpn. **81**, 011013 (2012).

[25] Y. Tanaka, K. Nakayama, S. Souma, T. Sato, N. Xu, P. Zhang, P. Richard, H. Ding, Y. Suzuki, P. Das, K. Kadowaki, and T. Takahashi, Phys. Rev. B **85**, 125111 (2012).

[26] A. Yamakage, K. Yada, M. Sato, and Y. Tanaka, Phys. Rev. B **85**, 180509(R) (2012).

[27] Y. Tanaka and S. Kashiwaya, Phys. Rev. Lett. **74**, 3451 (1995).

[28] S. Kashiwaya and Y. Tanaka, Rep. Prog. Phys. **63**, 1641 (2000).

[29] H.-J. Zhang, C.-X. Liu, X.-L. Qi, X.-Y. Deng, X. Dai, S.-C. Zhang, and Z. Fang, Phys. Rev. B **80**, 085307 (2009).

[30] C.-X. Liu, X.-L. Qi, H. J. Zhang, X. Dai, Z. Fang, and S.-C. Zhang, Phys. Rev. B **82**, 045122 (2010).

[31] R. Balian and N. R. Werthamer, Phys. Rev. **131**, 1553 (1963).

[32] A. I. Larkin, Sov. Phys. JETP Lett. **2**, 130 (1965).

[33] A. P. Mackenzie and Y. Maeno, Rev. Mod. Phys. **75**, 657 (2003).

[34] Y. Maeno, S. Kittaka, T. Nomura, S. Yonezawa, and K. Ishida, J. Phys. Soc. Jpn. **81**, 011009 (2012).

[35] P. W. Anderson, J. Phys. Chem. Solids **11**, 26 (1959).

[36] The magnetization was measured at several temperatures between 1.8 K and T_c of each sample. Before each run, the sample temperature was stabilized at 5 K ($>T_c$) and the magnet was quenched to remove any remnant field. Then the sample was cooled in zero field to the desired temperature and the magnetization was measured with increasing magnetic field.

[37] It has been found that n is nearly unchanged among various samples in the range of $0.1 \leqslant x \leqslant 0.5$ irrespective of the superconducting volume fraction, and hence it is most reasonable to infer that the local carrier density is essentially the same in superconducting and nonsuperconducting regions.

[38] R. A. Klemm, J. Low Temp. Phys. **39**, 589 (1980).

[39]V. G. Kogan, Phys. Rev. B **24**, 1572 (1981).

[40]J. R. Clem, Physica C **162**, 1137 (1989).

[41]A. L. Fetter and P. C. Hohenberg, in *Superconductivity*, edited by R. D. Parks (Dekker, New York, 1969), Vol. 2, Chap. 14.

[42]A. A. Abrikosov, Sov. Phys. JETP **5**, 1174 (1957).

[43]C.-R. Hu, Phys. Rev. B **6**, 1756 (1972).

[44]R. Liang, D. A. Bonn, W. N. Hardy, and D. Broun, Phys. Rev. Lett. **94**, 117001 (2005).

[45]The effective mass m^* was estimated for $x = 0.29$ from normal-state specific-heat data (Ref. 17) to be $m^* = 2.6m_e$ (m_e is the bare electron mass).

[46]This empirical formula is derived from the two-fluid model and is frequently used to fit the data of $\lambda^{-2}(T)$ $[\propto B_1(T)]$, since the differences between various limits are small [see M. Tinkham, *Introduction to Superconductivity*, 2nd ed. (McGraw-Hill, New York, 1996), p. 103].

[47]We have measured $M(B)$ curves in ± 1 T for $x = 0.16$, 0.29, and 0.40, and found that the pinning is always very weak with the irreversibility field of around 100 mT, which is essentially independent of x.

[48]E. H. Brandt, Phys. Rev. B **60**, 11939 (1999).

[49]Although $Cu_xBi_2Se_3$ samples are inhomogeneous, with the estimated size of the superconducting domains of 10–100 μm (Ref. 18), the characteristic domain size is much longer than the coherence length, and hence one can consider each superconducting domain to be a homogeneous superconductor [G. Deutscher, Physica B & C **109-110**, 1629 (1982)]. This justifies the use of the standard formulas for estimating various superconducting parameters.

[50]M. Ma and P. A. Lee, Phys. Rev. B **32**, 5658 (1985).

[51]A. V. Balatsky, I. Vekhter, and J.-X. Zhu, Rev. Mod. Phys. **78**, 373 (2006).

[52]J. L. Tallon, J. R. Cooper, S. H. Naqib, and J. W. Loram, Phys. Rev. B **73**, 180504(R) (2006).

[53]W. DeSorbo, Phys. Rev. **132**, 107 (1963).

[54]C. Egloff, A. K. Raychaudhuri, and L. Rinderer, J. Low Temp. Phys. **52**, 163 (1983).

[55]Since the superconducting $Cu_xBi_2Se_3$ exhibits only a single ellipsoidal Fermi surface around the Γ point (Ref. 19) and the electron correlations are expected to be weak due to the low-carrier-density nature, the free-electron model is a reasonable approximation for calculating the averaged k_F.

[56]Although the disorder increases with x, $k_F\ell$ is still much larger than 1 and hence $Cu_xBi_2Se_3$ is in the weakly disordered regime (Refs. 50 and 51). Also, the ratio ξ_0/ℓ is about 1 for $x \approx 0.26$ and hence $Cu_xBi_2Se_3$ is in between the clean and dirty limits.

[57]A. K. Raychaudhuri, C. Egloff, and L. Rinderer, J. Low Temp. Phys. **53**, 513 (1983).

[58]M. Tinkham, Ref. 46, Chap. 3.10.4.

[59]For our calculation of $\lambda_{BCS}(0)$ expected for BCS superconductors, we used the BCS gap value $\Delta_0 = 1.764k_BT_c^0$ with the clean-limit critical temperature T_c^0 which we identify with the maximum T_c of 3.8 K in $Cu_xBi_2Se_3$.